Realization of Spin Gapless Semiconductors: The Heusler Compound Mn_2CoAl

Siham Ouardi, Gerhard H. Fecher,[*] and Claudia Felser

Max Planck Institute for Chemical Physics of Solids, D-01187 Dresden, Germany

Jürgen Kübler

Institut für Festkörperphysik, Technische Universität Darmstadt, D-64289 Darmstadt, Germany

Recent studies have reported an interesting class of semiconductor materials that bridge the gap between semiconductors and half-metallic ferromagnets. These materials, called spin gapless semiconductors, exhibit a band gap in one of the spin channels and a zero band gap in the other and thus allow for tunable spin transport. Here, we report the first experimental verification of the spin gapless magnetic semiconductor Mn_2CoAl, an inverse Heusler compound with a Curie temperature of 720 K and a magnetic moment of $2\mu_B$. Below 300 K, the compound exhibits nearly temperature-independent conductivity, very low, temperature-independent carrier concentration, and a vanishing Seebeck coefficient. The anomalous Hall effect is comparatively low, which is explained by the symmetry properties of the Berry curvature. Mn_2CoAl is not only suitable material for room temperature semiconductor spintronics, the robust spin polarization of the spin gapless semiconductors makes it very promising material for spintronics in general.

Recent studies have reported on an interesting class of materials, namely, spin gapless semiconductors [1]. Spin gapless semiconductivity was predicted in diluted magnetic semiconductors. Since the precondition for semiconductor spintronics is ferromagnetic semiconductors, diluted semiconductors are the subject of intense research. However, their drawback is the low Curie temperature T_c of at most 180 K [2,3].

Heusler compounds are known for their exceptional tunability and high Curie temperature. Indeed, the realization of materials that fulfill the needs for semiconductor spintronics is possible, and even the design of spin gapless semiconductors is achieved in the new class of manganese-rich Heusler compounds. Mn_2-Heusler compounds can also be designed as half-metallic magnets similar to Co_2-Heusler compounds [4].

In all half-metallic materials, transport is mediated by electrons having only one kind of spin, since the electronic structure is metallic in one spin direction. Here we show that in Mn-rich Heusler compounds, the realization of band gaps in both spin directions is possible. Spin gapless semiconductors exhibit an additional phenomenon, namely, an open band gap in one spin channel and a closed gap in the other. The principle density of states scheme for half-metallic ferromagnets is compared with spin gapless semiconductors in Fig. 1.

Many of the Co_2- and Mn_2-Heusler compounds are ferromagnetic and ferrimagnetic half-metals. The Fermi energy intersects the majority spin density [Fig. 1(a)]. The class of spin gapless semiconductors appears if the conduction and valence band edges of the majority electrons touch at the Fermi energy ϵ_F [Fig. 1(b)]. This class is

thus an important subclass of zero band gap insulators or gapless semiconductors [5]. In zero band gap materials, no threshold energy is required to move electrons from occupied states to empty states. Therefore, these materials exhibit unique properties, as their electronic structure is extremely sensitive to external influences [5]. Many of the known gapless semiconductors exhibit a so-called inverted band structure [5,6], and, thus, they act as topological insulators [7,8]. In spin gapless semiconductors, not only the excited electrons but also the holes can be 100% spin polarized. This results in unique transport properties: the coexistence of high resistance and high Curie temperature, as well as a small anomalous Hall effect in spite of a large magnetic moment.

The new Heusler compound for which we found the required electronic structure is Mn_2CoAl, whose physical properties are investigated in this Letter. The compound
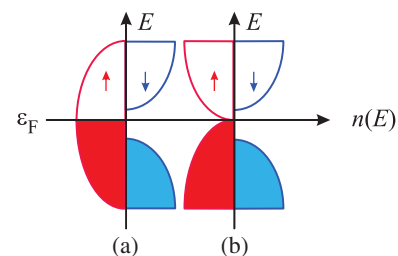
FIG. 1 (color). Density of states schemes. The schematic density of states $n(E)$ as a function of energy E is shown for (a) a half-metallic ferromagnet and (b) a spin gapless semiconductor. The occupied states are indicated by filled areas. Arrows indicate the majority ($\uparrow$) and minority ($\downarrow$) states.

crystallizes in the inverse Heusler structure with space group $F\bar{4}3m$ and Wyckoff sequence $acbd$ for the atoms Mn-Mn-Co-Al. To explain the electronic structure and magnetic properties, *ab initio* calculations were performed using different methods [9,10]. The results are in agreement with previous calculations, especially concerning the size of the spin gap. The Berry curvature and the anomalous Hall conductivity were computed using the fast augmented spherical wave density functional method [11]. The technical details of such calculations have been reported in Ref. [12].

Figure 2 shows the scalar-relativistic band structure of Mn$_2$CoAl. The calculations were also performed with spin-orbit interaction respected for all atoms as this is essential for the Berry curvature calculations reported below. The electronic structures obtained with and without spin-orbit interaction are very similar [9]. It is obvious that this electronic structure of the magnetic semiconductor Mn$_2$CoAl is unique. There are many nonmagnetic semiconductors in the family of the Heusler compounds that can be identified by electron-counting rules [13], such as Fe$_2$VAl [14]. Here the band structure and the band gap are different for each spin channel. Indeed, the spin character of the bands close to the Fermi energy is pure even though the spin orbit interaction mixes, in general, states with different spin projections. Obviously, the band structure exhibits the expected semiconducting magnetic character with a band gap in the minority states (blue). The gap between t_{2g} and e_g states occurs at Γ and is similar also to the band structure of the nonmagnetic semiconductor Fe$_2$VAl. We emphasize that band structure is different in the majority channel (red). The gap is indirect, the valence band at Γ touches the conduction band at X, and the magnetism occurs due to the band inversion of the e_g band indicated in Fig. 2. Therefore, the magnetic moment is calculated to be $2\mu_B$, in excellent agreement with the experiment (see below). The site-resolved spin magnetic
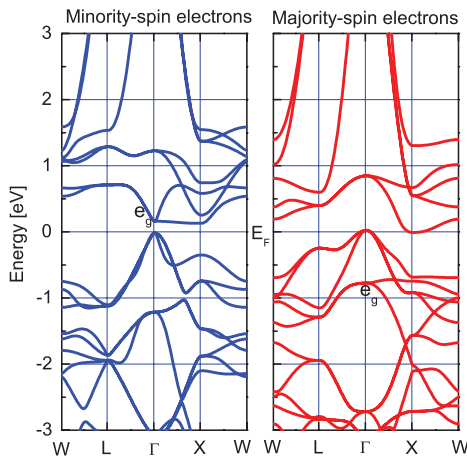
moments are approximately $m_{Mn(4a)} = -2\mu_B$, $m_{Co(4b)} = +1\mu_B$, and $m_{Mn(4c)} = +3\mu_B$, confirming a ferrimagnetic character with antiparallel coupling of the moments at the neighboring Mn sites. In the following it will be shown that various extraordinary physical properties are in agreement with the proposed behavior as spin gapless semiconductor.

Polycrystalline Mn$_2$CoAl was prepared by arc melting. The resulting ingots were annealed at different temperatures under argon in quartz ampules. The annealing was followed by fast cooling to 273 K (quenching in ice water). The crystalline structure, homogeneity, and composition of the samples were checked by XRD and energy-dispersive x-ray spectroscopy. No impurities or inhomogeneities were detected by energy-dispersive x-ray spectroscopy. Transport measurements were performed by means of a physical properties measurement system (PPMS, Quantum Design). For transport measurements, samples of $(2 \times 2 \times 8)$ mm^3 were cut from the ingots. The temperature was varied from 1.8 to 350 K. The Hall effect of the compound was measured in the temperature range from 5 to 300 K in magnetic induction fields from -9 to $+9$ T. The Hall coefficient was calculated from the slope of the measured Hall coefficient R_H. The carrier concentration $n = 1/eR_H$ was extracted from R_H using a single band model [15] (e is the elementary electron charge). The temperature dependence of the magnetization was measured from 4.8 to 800 K using a magnetic properties measurement system (MPMS, Quantum Design). For these measurements, small sample pieces of approximately 8 mg were used. The experiments on Mn$_2$CoAl confirmed that it crystallizes in the expected crystalline structure. Powder XRD revealed single phased samples with inverse Heusler structure and a lattice parameter of $a = 5.798$ Å for the postannealed samples. The saturation magnetic moment is $2\mu_B$ at low temperature ($T < 5$ K) [see inset (b) in Fig. 5] and the compound has a Curie temperature of 720 K [Fig. 5(c)].

The temperature dependencies of electrical conductivity $\sigma(T)$, Seebeck coefficient $S(T)$, and carrier concentration $n(T)$ of Mn$_2$CoAl are shown in Fig. 3. The conductivity $\sigma(T)$ clearly exhibits a nonmetallic behavior being rather of semiconducting type: It increases with increasing temperature and a value of about 2440 S/cm is obtained at 300 K. As shown in Fig. 3(b), the Seebeck coefficient $S(T)$ nearly vanishes in the temperature range from 5 to 150 K and adopts a very low value of only about 2 μV/K at 300 K, untypically for a semiconductor. From measurement of the Hall coefficient one reveals a very low carrier concentration of only 2×10^{17} cm^{-3} at 300 K. It is also nearly constant with temperature and approaches a value as low as 1.3×10^{17} cm^{-3} at 2 K. It is stressed here that all synthesized samples show high resistance, low charge-carrier concentration, and low Seebeck coefficients, which demonstrates the exceptional stability of the electronic structure and the insensitivity to disorder of this compound. This is in contrast to the Co$_2$-Heusler compounds,

FIG. 2 (color).   Band structure of Mn$_2$CoAl.
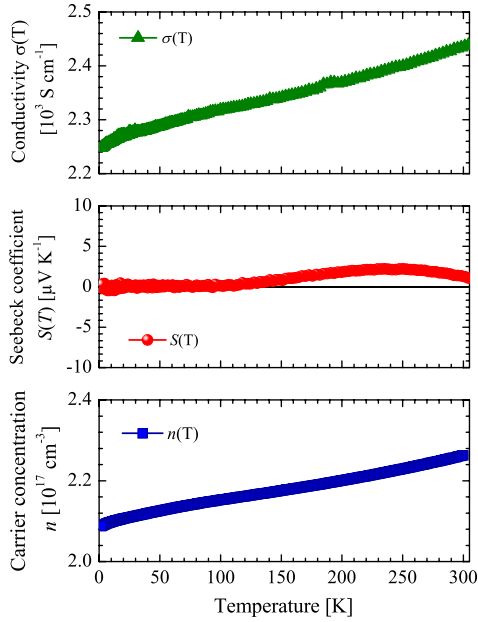
FIG. 3 (color online).   Temperature dependence of conductivity $\sigma_{xx}(T)$, Seebeck coefficient $S(T)$, and carrier concentration $n(T)$ of Mn_2CoAl.

FIG. 4 (color online).   Magnetoresistance of Mn_2CoAl measured at different temperatures.

widely studied for spintronics, for which it is known that disorder destroys the half-metallicity.

The linear temperature coefficient of the conductivity is $-1.4 \times 10^{-9} \; \Omega \cdot m/K$ and nearly independent of temperature up to 300 K. This behavior is remarkable and not comparable to those of regular metals or semiconductors, which exhibit exponential increases or decreases in conductivity. As Mn_2CoAl is a well-ordered compound without antisite disorder, this behavior cannot be attributed to impurity scattering. A similar, linear behavior of the resistance was also reported for half-metallic ferromagnets, but only at low temperatures [16]. The resistivity in those metallic systems ($< 0.5 \; \mu\Omega \cdot m$ for PtMnSn) is, however, 3 orders of magnitude lower than that of Mn_2CoAl ($\approx 400 \; \mu\Omega \cdot m$). The temperature-independent charge-carrier concentration is typical for gapless systems [5]. The value observed here is of the same order as that observed for quantum well structures of HgCdTe ($10^{15}–10^{17} \; cm^{-3}$) and significantly lower than that for Fe_2VAl ($10^{21} \; cm^{-3}$) [17], a proposed semiconducting Heusler compound. The vanishing Seebeck effect over a wide range of temperatures as a result of electron and hole compensation is remarkable. Different samples with different resistivities ($0.8–6 \; \mu\Omega \cdot m$) always show a nearly zero Seebeck coefficient.

So far, the electronic transport properties, together with the predicted and measured magnetic moment of $2\mu_B$, strongly support the view that Mn_2CoAl is a spin gapless semiconductor. To investigate further transport properties of the spin gapless state, the magnetoresistance (MR) and anomalous Hall conductivity of Mn_2CoAl were measured.

The results of the MR measurements at different temperatures are displayed in Fig. 4, and show a remarkable effect. A change of sign appears at around 150 K, below which the Seebeck effect vanishes. Above 200 K, the MR is low and exhibits a negative, saturating dependence on the applied magnetic field. At lower temperatures, the MR becomes positive and reaches a value of about 10% at 2 K for an induction field of 9 T. The low-temperature MR is clearly nonsaturating and nearly linear, even in high fields. Above 1 T, its derivative has an approximately constant value of $10^{-4} \; T^{-1}$ at 2 K. Various gapless semiconductors have already been shown to exhibit such a quantum linear MR [18] in very small transverse magnetic fields.

The anomalous Hall conductivity $\sigma_{xy} = \frac{\rho_{xy}}{\rho_{xx}^2}$ was extracted from the magnetic field-dependent transport measurements to disentangle the low-field behavior in more detail. The result is shown in Fig. 5. $\sigma_{xy}(H)$ follows the field dependence of the magnetization $m(H)$ [inset (b) of Fig. 5]. The anomalous Hall conductivity σ_{xy0} has a very low value of 22 S/cm at 2 K. This value is about 20–100 times smaller than those of half-metallic Heusler compounds [19] and ferromagnetic metals [20], which is surprising in the context of the high magnetic moment and the high Curie temperature.

The anomalous Hall effect was calculated using the Berry-phase approach [12] in order to explain its extraordinarily small value. The result of the calculation is shown in Fig. 6. The symmetry of the Berry curvature $\Omega_z(\mathbf{k})$ in a plane of the Brillouin zone is clearly visible. This pattern symmetry is different from the patterns of regular ferromagnets (e.g., compare Fe [20]). Moreover, it is easily seen that the pattern for momentum vectors with the opposite sign (here at $k_z = \pm 0.25$) is nearly antisymmetric. The anomalous Hall conductivity is given by a Brillouin
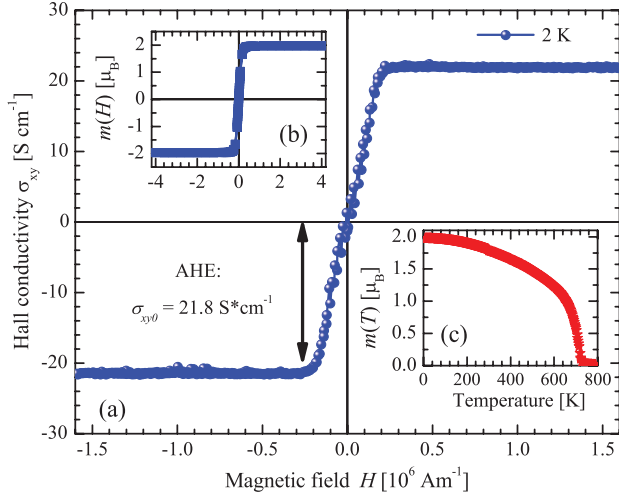
FIG. 5 (color).   Magnetic properties and anomalous Hall effect (AHE) of Mn_2CoAl. The Hall conductivity σ_{xy} is shown as a function of the applied magnetic field. The anomalous Hall effect is defined by the difference between σ_{xy} values in zero and saturation fields (≈ 0.3 T). Inset (a) shows the hysteresis $m(H)$ measured at 2 K. Inset (b) shows the temperature dependence of the magnetization $m(T)$ measured in a field of 1 T.

zone integral over the Berry curvature $\Omega_z(\mathbf{k})$ over all occupied states [20]:

$$\sigma_{xy} = \frac{e^2}{h} \int \frac{d\mathbf{k}}{(2\pi)^d} \Omega_z(\mathbf{k}) f(\mathbf{k}), \qquad (1)$$

where $f(\mathbf{k})$ is the Fermi distribution function (at $T = 0$) and the dimension $d = 3$. This makes clear that the nearly vanishing anomalous Hall effect of Mn_2CoAl arises from the antisymmetry of the Berry curvature for k_z vectors of opposite sign. Indeed, a numerical integration of Eq. (1) gives $\sigma_{xy} = 3$ S/cm, which is lower than the experimental value. This small value comes from positive and negative contributions of about 150 S/cm each. The small switching field used in the experiment could therefore account for the difference between the calculated and the experimental values.
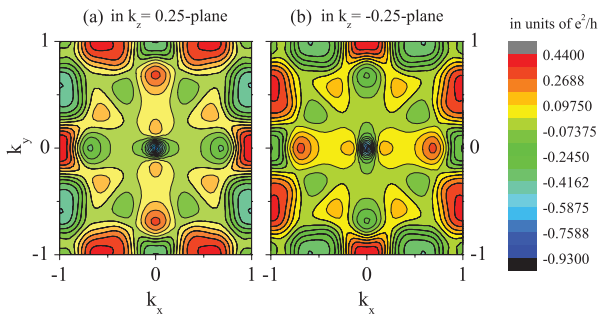
FIG. 6 (color).   Berry curvature in the $k_z = 0.25$ plane (a) and $k_z = -0.25$ plane (b) for Mn_2CoAl.

We conclude that the Heusler compound Mn_2CoAl is a spin gapless semiconductor, as suggested by *ab initio* calculations. This unique class of materials will have a considerable impact on the field of spintronics as it opens up new and advanced possibilities for physical phenomena and devices based on spin transport. In spin gapless materials, only one spin channel contributes to the transport properties, whereas the other spin channel allows for tunable charge-carrier concentrations. In the present work, Mn_2CoAl has been synthesized and its spin gapless state has been verified for the first time. Its crystalline structure is of the inverse Heusler type. The saturation magnetic moment is $2\mu_B$ at 5 K, and the Curie temperature of 720 K makes it suitable for room temperatures applications. The magnetic semiconductor Mn_2CoAl may serve as a spin injector into semiconductors. Mn_2CoAl is even a spin gapless semiconductor with nearly temperature-independent, low conductivity of the order of 2×10^5 S/m, and a low charge-carrier concentration of the order of 10^{17} cm^{-3}, as well as a vanishing Seebeck coefficient. Therefore, the high spin polarization is expected also in the excited state and thus makes this Heusler compound an ideal material for spin-Seebeck investigations and for spintronics in general. The temperature dependence of the MR is nontrivial; below 150 K it shows the typical quantum MR of a spin gapless semiconductor. The low value of the anomalous Hall effect of 22 S/cm at 2 K which is in good agreement with the Berry curvature calculation is also remarkable.

*fecher@cpfs.mpg.de
[1] X. L. Wang, Phys. Rev. Lett. **100**, 156404 (2008).
[2] H. Ohno, Science **281**, 951 (1998).
[3] M. Wang, R. P. Campion, A. W. Rushforth, K. W. Edmonds, C. T. Foxon, and B. L. Gallagher, Appl. Phys. Lett. **93**, 132103 (2008).
[4] J. Kübler, A. R. Williams, and C. B. Sommers, Phys. Rev. B **28**, 1745 (1983).
[5] I. M. Tsidilkovski, *Electron Spectrum of Gapless Semiconductors*, Springer Series in Solid-State Sciences Vol. 116 (Springer, Berlin, New York, 1996).
[6] S. H. Groves, R. N. Brown, and C. R. Pidgeon, Phys. Rev. **161**, 779 (1967).
[7] S. Murakami, N. Nagaosa, and S.-C. Zhang, Phys. Rev. Lett. **93**, 156804 (2004).
[8] C. L. Kane and E. J. Mele, Phys. Rev. Lett. **95**, 146802 (2005).
[9] G. D. Liu, X. F. Dai, H. Y. Liu, J. L. Chen, Y. X. Li, G. Xiao, and G. H. Wu, Phys. Rev. B **77**, 014424 (2008).

P H Y S I C A L   R E V I E W   L E T T E R S

[10] N. Xing, H. Li, J. Dong, R. Long, and C. Zhang, Comput. Mater. Sci. **42,** 600 (2008).

[11] A. R. Williams, J. Kübler, and C. D. Gelatt, Phys. Rev. B **19,** 6094 (1979).

[12] J. Kübler and C. Felser, Phys. Rev. B **85,** 012405 (2012).

[13] T. Graf, C. Felser, and S. S. P. Parkin, Prog. Solid State Chem. **39,** 1 (2011).

[14] H. Okamura, J. Kawahara, T. Nanba, S. Kimura, K. Soda, U. Mizutani, Y. Nishino, M. Kato, I. Shimoyama, H. Miura, K. Fukui, K. Nakagawa, H. Nakagawa, and T. Kinoshita, Phys. Rev. Lett. **84,** 3674 (2000).

[15] D. M. Rowe, *Thermoelectrics Handbook: Macro to Nano* (CRC/Taylor & Francis, Boca Raton, FL, 2006), lst ed.

[16] J. S. Moodera and D. M. Mootoo, J. Appl. Phys. **76,** 6101 (1994).

[17] V. I. Okulov, V. E. Arkhipov, T. E. Govorkova, A. V. Korolev, and K. A. Okulova, Low Temp. Phys. **33,** 692 (2007).

[18] A. A. Abrikosov, Phys. Rev. B **58,** 2788 (1998).

[19] D. Bombor, C. G. F. Blum, O. Volkonskiy, S. Rodan, S. Wurmehl, C. Hess, and B. Büchner, Phys. Rev. Lett. **110,** 066601 (2013).

[20] Y. Yao, L. Kleinman, A. H. MacDonald, J. Sinova, T. Jungwirth, D.-s. Wang, E. Wang, and Q. Niu, Phys. Rev. Lett. **92,** 037204 (2004).